Golgi complex–plasma membrane trafficking directed by an autonomous, tribasic Golgi export signal

Hirendrasinh B. Parmar[a,*], Christopher Barry[a,*], FuiBoon Kai[a], and Roy Duncan[a,b,c]
[a]Department of Microbiology and Immunology, [b]Department of Biochemistry and Molecular Biology, and [c]Department of Pediatrics, Dalhousie University, Halifax, NS B3H 4R2, Canada

ABSTRACT **Although numerous linear motifs that direct protein trafficking within cells have been identified, there are few examples of linear sorting signals mediating directed export of membrane proteins from the Golgi complex to the plasma membrane. The reovirus fusion-associated small transmembrane proteins are simple, single-pass transmembrane proteins that traffic through the endoplasmic reticulum–Golgi pathway to the plasma membrane, where they induce cell–cell membrane fusion. Here we show that a membrane-proximal, polybasic motif (PBM) in the cytosolic tail of p14 is essential for efficient export of p14 from the Golgi complex to the plasma membrane. Extensive mutagenic analysis reveals that the number, but not the identity or position, of basic residues present in the PBM dictates p14 export from the Golgi complex, with a minimum of three basic residues required for efficient Golgi export. Results further indicate that the tribasic motif does not affect plasma membrane retention of p14. Furthermore, introduction of the tribasic motif into a Golgi-localized, chimeric ERGIC-53 protein directs export from the Golgi complex to the plasma membrane. The p14 PBM is the first example of an autonomous, tribasic signal required for Golgi export to the plasma membrane.**

Monitoring Editor
Adam Linstedt
Carnegie Mellon University

Received: Jul 5, 2013
Revised: Nov 26, 2013
Accepted: Jan 16, 2014

INTRODUCTION

Integral membrane proteins, which comprise approximately one-third of the proteins in the human proteome, must be sorted and localized to spatially segregated membrane compartments (Almen *et al.*, 2009; Pandey, 2010). Integral membrane proteins that depend on the secretory pathway for trafficking to the correct subcellular compartment generally use a signal peptide to direct cotranslational insertion of the protein into the endoplasmic reticulum (ER) membrane (Zimmermann *et al.*, 2011). After transport through the ER–Golgi complex vesicle transport pathway to the *trans*-Golgi network (TGN), frequently accompanied by posttranslational modification, these membrane proteins must then be sorted and directed to their final membrane destination. Although numerous *cis* and *trans* factors that regulate protein trafficking have been defined, our understanding of this process, particularly as it relates to exit from the Golgi complex to the plasma membrane, is far from complete.

Efficient export of membrane proteins from the ER is a directed process mediated by coat protein (COP) II–coated transport vesicles and facilitated by ER export signals present in the protein being transported. COPII vesicle assembly is regulated by the small GTPase Sar1, which recruits the heterodimeric Sec23/24 adaptor protein complex and the Sec13/31 cage complex (Barlowe, 2003; Gurkan *et al.*, 2006; Zanetti *et al.*, 2011). Transmembrane cargo proteins containing specific ER export signals interact with components of the COPII complex and are concentrated at specific ER export sites where vesicle formation occurs in conjunction with cargo selection (Nishimura *et al.*, 1999; Votsmeier and Gallwitz, 2001; Miller *et al.*, 2003; Farhan *et al.*, 2007; Stagg *et al.*, 2008). Several different ER export signals have been identified in a diverse range of membrane proteins (Barlowe, 2003). For example, conserved hydrophobic

This article was published online ahead of print in MBoC in Press (http://www.molbiolcell.org/cgi/doi/10.1091/mbc.E13-07-0364) on January 22, 2014.

*These authors contributed equally to this study.

Address correspondence to: Roy Duncan (roy.duncan@dal.ca).

Abbreviations used: AP, adaptor protein; COP, coat protein; endo H, endoglycosidase H; ER, endoplasmic reticulum; FAST, fusion-associated small transmembrane; HBSS, Hank's balanced salt solution; HRP, horseradish peroxidase; PBM, polybasic motif; PDI, protein disulfide isomerase; PI4KIIIβ, phosphatidylinositol-4 kinase-IIIβ; PNGase F, N-glycosidase F; TGN, *trans*-Golgi network; TMD, transmembrane domain.

sequences in the cytosolic tail of G protein–coupled receptors and glycosylation signals in the luminal domain or sequences within the transmembrane domain (TMD) of ERGIC-53 probably influence ER exit by affecting protein folding or multimerization (Nufer *et al.*, 2003; Duvernay *et al.*, 2009). Numerous linear ER export signals have also been identified. These export signals, located in the cytosolic tails of integral membrane proteins destined for ER exit, include diacidic, dibasic, tribasic, or tyrosine-based hydrophobic motifs. In several instances, ER exit is based on interactions between the linear export signals and the Sec24 component of the COPII complex (Nishimura and Balch, 1997; Sevier *et al.*, 2000; Giraudo and Maccioni, 2003; Zhang *et al.*, 2011; Dong *et al.*, 2012).

As with exit from the ER, it is now recognized that linear sorting signals also mediate trafficking of membrane proteins from the Golgi complex to their final membrane compartment, with most of this sorting occurring in the TGN (Anitei and Hoflack, 2011). Membrane proteins exiting the Golgi complex must be sorted to numerous membrane destinations in discrete regions of the plasma membrane and endocytic compartments. Sorting at the TGN therefore requires a multitude of distinct vesicle carriers and divergent trafficking pathways (Bonifacino and Traub, 2003). Examples include the heterotetrameric adaptor protein (AP) complexes and Golgi-localizing, γ-adaptin ear homology domain (GGA) proteins that sort Golgi cargo into different vesicle carriers (De Matteis and Luini, 2008). In the case of APs, they recognize two well-characterized classes of sorting signals that comprise short, linear, degenerate amino acid sequence motifs present in the cytosolic tails of membrane proteins exiting the Golgi complex. The tyrosine-based signals have an NPXY or YXXϕ (X is any amino acid, ϕ is a bulky hydrophobic residue) consensus sequence, whereas dileucine motifs are often contained within [DE]XXXL[LI] or DXXLL consensus sequences (Rodriguez-Boulan and Musch, 2005). These Golgi sorting signals may be more complex and can also function as sorting signals at other membrane compartments. For example, the YTDIE signal in vesicular stomatitis G protein functions as both a tyrosine- and diacidic-based sorting signal for export from both the ER and the Golgi (Nishimura and Balch, 1997; Sevier *et al.*, 2000; Nishimura *et al.*, 2002). Sequence features in the vicinity of these Golgi sorting signals can also exert an effect, as exemplified by the YIPL motif in the Kir2.1 inwardly rectifying potassium channel, whose Golgi export activity is strongly influenced by undefined flanking sequences (Hofherr *et al.*, 2005). For the most part, the identified Golgi trafficking signals are not required for Golgi export but instead serve as sorting signals for directed trafficking to a specified membrane compartment.

The reovirus fusion-associated small transmembrane (FAST) proteins are a family of bitopic transmembrane proteins encoded by the fusogenic orthoreoviruses and aquareoviruses, a diverse group of nonenveloped viruses in the family *Reoviridae* (Duncan, 1999). The FAST proteins are the only example of membrane fusion proteins encoded by nonenveloped viruses, are the smallest known membrane protein fusogens (95–198 residues), and are directly responsible for the ability of the fusogenic reoviruses to induce syncytium formation (Boutilier and Duncan, 2011). There are six members of the FAST protein family, each encoded by different species of fusogenic reoviruses, which are named according to their predicted molecular mass: p10, p13, p14, p15, p16, and p22 (Shmulevitz and Duncan, 2000; Dawe and Duncan, 2002; Corcoran and Duncan, 2004; Racine *et al.*, 2009; Thalmann *et al.*, 2010; Guo *et al.*, 2013). In the absence of an N-terminal signal peptide, the FAST proteins use their single TMD as a reverse signal anchor to direct $N_{exoplasmic}$/$C_{cytoplasmic}$ insertion into the ER membrane (Shmulevitz and Duncan, 2000; Corcoran and Duncan, 2004; Dawe *et al.*, 2005). The FAST proteins are then trafficked through the secretory pathway to the plasma membrane, where their sole defined function is to induce cell–cell membrane fusion (Shmulevitz *et al.*, 2004; Dawe *et al.*, 2005; Corcoran *et al.*, 2011). The mechanisms governing transport of these simple, single-pass membrane proteins to the plasma membrane have not been investigated.

We exploited the simple structure of the FAST proteins to determine the nature of *cis*-acting factors that regulate plasma membrane localization. The 125-residue p14 FAST protein contains a single TMD flanked by a 36-residue myristoylated, N-terminal ectodomain and a 68-residue C-terminal cytosolic domain (Corcoran and Duncan, 2004). Mutational studies indicated that a juxtamembrane polybasic motif (PBM) contained within the cytosolic tail of p14 is essential for plasma membrane localization. This PBM is not required for ER exit but is required for p14 export from the Golgi complex, with a minimum of three basic residues in proximity to the membrane determining the ability of the PBM to function as an efficient Golgi export signal. Moreover, transfer of the PBM to a heterologous, Golgi-resident transmembrane protein directs plasma membrane localization, indicating that this novel tribasic motif is both necessary and sufficient to mediate Golgi export of membrane proteins to the plasma membrane.

RESULTS

The polybasic motif is required for p14 localization to the plasma membrane

All of the FAST proteins contain a membrane-proximal cluster of three to eight basic residues in their cytosolic C-terminal endodomains. Previous substitution analysis of the PBM of the p10 and p15 FAST proteins indicated that this motif is required for cell–cell fusion (Shmulevitz *et al.*, 2003; Dawe *et al.*, 2005), although the basis for this loss of fusion activity was not determined. The seven-residue p14 PBM resides four residues downstream of the TMD and comprises two tribasic clusters separated by an acidic residue (KRRERRR). To examine the importance of the p14 PBM, we replaced the two tribasic clusters by Ala, either individually (constructs p14-KRR and p14-RRR) or in combination (construct p14-PB; Figure 1A). These constructs were transfected into QM5 cells and examined for syncytiogenesis by microscopic examination of Giemsa-stained monolayers (Figure 1B), and the extent of syncytium formation was determined by quantifying the numbers of syncytial nuclei in random microscopic fields (Figure 1C). The p14-KRR and p14-RRR constructs showed slightly reduced levels of syncytium formation relative to authentic p14, whereas the p14-PB construct containing Ala substitutions of all six basic residues was devoid of cell–cell fusion activity. All three of the Ala constructs were expressed at approximately equivalent levels as authentic p14 (Figure 1D), although p14-PB showed a trend to slightly lower (~20–40% decrease) expression levels in multiple Western blots. These modest and variable difference in p14-PB expression did not correlate with the consistent loss of syncytium formation, indicating that the p14 PBM is essential for fusion activity independent of effects on p14 expression.

To determine the basis for the syncytiogenic defect in the p14-PB construct, we assessed cell surface expression of p14-PB by fluorescence-activated cell sorting (FACS) analysis using an antiserum specific for the p14 ectodomain to stain live cells. The p14 FAST protein induces very rapid and robust syncytium formation in QM5 cells, which commences 4 h posttransfection (hpt) and encompasses the entire monolayer by 12 hpt (Salsman *et al.*, 2005). The p14 antiserum was therefore added to cells 3 hpt to inhibit syncytium formation, allowing extended incubations to increase the

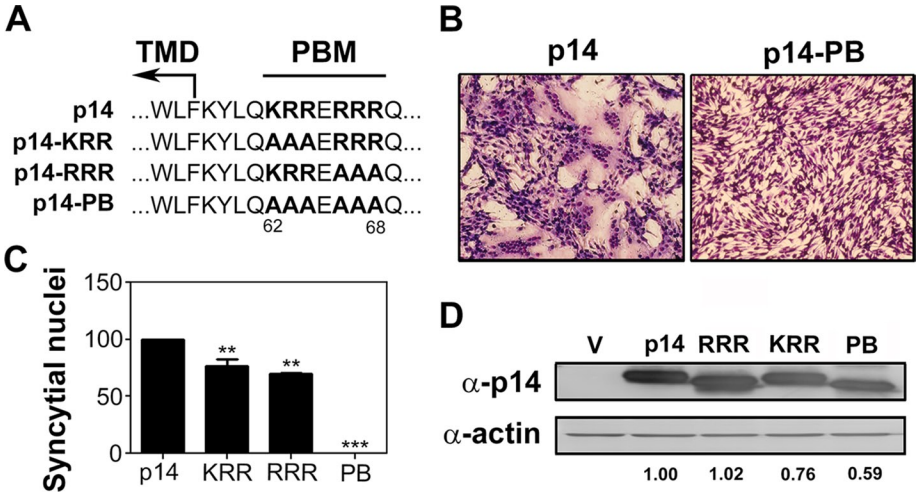

FIGURE 1: The p14 PBM is required for cell–cell fusion. (A) Amino acid sequence of the p14 PBM and the indicated polybasic mutants. Numbers indicate residue position in p14. Boundary of the TMD and location of the PBM are indicated. (B) QM5 cells transfected with p14 or p14-PB were Giemsa stained at 8 hpt and imaged by bright-field microscopy at 200× magnification. (C) QM5 cells transfected with p14 or the indicated polybasic mutants (p14-KRR [KRR], p14-RRR [RRR], or p14-PB [PB]) were imaged as in B, and syncytial nuclei were quantified from five random fields. Results are mean number of syncytial nuclei ± SEM from two independent experiments performed in triplicate. Statistical significance relative to p14 (**$p < 0.01$; ***$p < 0.005$). (D) Lysates of QM5 cells transfected with the indicated p14 constructs as in C were processed for Western blotting at 8 hpt using anti-p14 or anti-actin antibody. Numbers at the bottom indicate relative band intensity normalized to p14.

detection and quantification of cell surface fluorescence, as previously described (Barry and Duncan, 2009; Barry *et al.*, 2010). Replacement of three of the six basic residues in the PBM (constructs p14-KRR and p14-RRR) led to no significant reduction in p14 plasma membrane localization (Figure 2C), indicating that the slight reduction in syncytiogenesis induced by these constructs (Figure 1C) reflects an effect on fusion activity, not trafficking, of p14. In contrast, Ala replacement of all six basic residues in the PBM abrogated syncytium formation (Figure 1) and decreased p14-PB cell surface expression by >95% (Figure 2, A and C). FACS analysis using permeabilized cells to detect total expression levels revealed <20% decrease in p14-PB expression (Figure 2, B and D), similar to Western blotting results (Figure 1D), implying that the dramatic inhibition of p14-PB plasma membrane localization was not due to effects on protein expression. Because basic residues on the cytosolic side of a TMD influence protein topology—the so-called "positive inside rule" (Nilsson *et al.*, 2005)—flow cytometry was also performed using antiserum raised against full-length p14. This antiserum has high affinity for epitopes in the C-terminal p14 cytosolic domain (Clancy and Duncan, 2009) but still failed to detect p14-PB on the cell surface (Figure 2E). Basic residues in the p14 PBM therefore do not affect p14 topology in the membrane but are required for p14 trafficking to the plasma membrane.

The polybasic motif is not required for p14 export from the ER

Basic residues in the cytosolic tails of some membrane proteins can promote ER export (Dong *et al.*, 2012). To determine whether the absence of the p14-PB construct in the plasma membrane reflected an inability to traffic from ER to the Golgi complex, we introduced a V9T substitution into p14-PB. Previous results using endoglycosidase H (endo H) in the presence and absence of the N-linked glycosylation inhibitor tunicamycin demonstrated this substitution creates a functional glycosylation signal in p14 (Corcoran and Duncan, 2004). FACS analysis of cell surface fluorescence indicated that this glycosylation signal does not inhibit, and might actually slightly enhance, p14(V9T) plasma membrane localization (Figure 3A). Western blots of lysates from QM5 cells transfected with p14(V9T) detected two p14 polypeptides (Figure 3B). Treatment of cell lysates with N-glycosidase F (PNGase F), an amidase that cleaves both high-mannose and complex N-linked carbohydrates from glycoproteins, confirmed that the slower-migrating species was glycosylated p14 (Figure 3B). The slower-migrating species was also partially resistant to treatment with endo H, indicative of processing in the Golgi complex to an endo H–resistant complex oligosaccharide. A similar situation was observed for p14-PB(V9T), with the presence of a slower-migrating, partially endo H–resistant polypeptide (Figure 3B). Absence of the PBM in p14-PB(V9T) led to no significant difference in the proportion of endo H–resistant p14-PB(V9T) relative to p14(V9T) (Figure 3C), indicating that the PBM is not required for p14 ER–Golgi trafficking.

The p14 PBM functions as a Golgi export signal

The endo H and surface expression results indicated that p14-PB traffics to the Golgi complex but fails to traffic to the plasma membrane, suggesting that the PBM might function as a Golgi export signal. To test this hypothesis, we examined the influence of the PBM on p14 subcellular localization by immunofluorescence microscopy, using Vero cells transfected with p14(V9T) constructs. The p14(V9T) construct correctly traffics to the plasma membrane (Figure 3A) but is fusion dead due to the Val–Thr substitution, which allowed longer incubations without the need to inhibit syncytium formation using high concentrations of α-p14 antiserum. The flatter, larger, and more uniform morphology of Vero cells provided better visualization of cytosolic compartments than in QM5 cells and provided a means to assess whether the PBM exerts any cell-specific trafficking effects. The p14(V9T) construct displayed disseminated intracellular fluorescence throughout the cytoplasm that radiated out to the cell periphery, with little indication of p14 concentration in the Golgi complex (Figure 4, top row). In contrast, p14-PB(V9T) showed a very faint, diffuse cytoplasmic staining pattern with no evidence of staining at the cell periphery (Figure 4). The p14-PB(V9T) construct strongly colocalized with phosphatidylinositol-4 kinase-IIIβ (PI4KIIIβ), a Golgi complex marker, and with TGN46; this colocalization was obvious, reproducible between experiments, and apparent in almost all cells expressing p14-PB(V9T). Absence of the PBM therefore results in p14 accumulation in the Golgi complex and TGN and inability of p14 to traffic to the plasma membrane.

Accumulation of p14-PB in the Golgi complex could reflect either failure to exit the Golgi complex or rapid retrieval of p14 from the plasma membrane to the Golgi complex via the endocytic pathway. To distinguish between these possibilities, we inhibited dynamin-dependent endocytic events using dynasore, a dynamin inhibitor (Kirchhausen *et al.*, 2008). We used the nonfusogenic

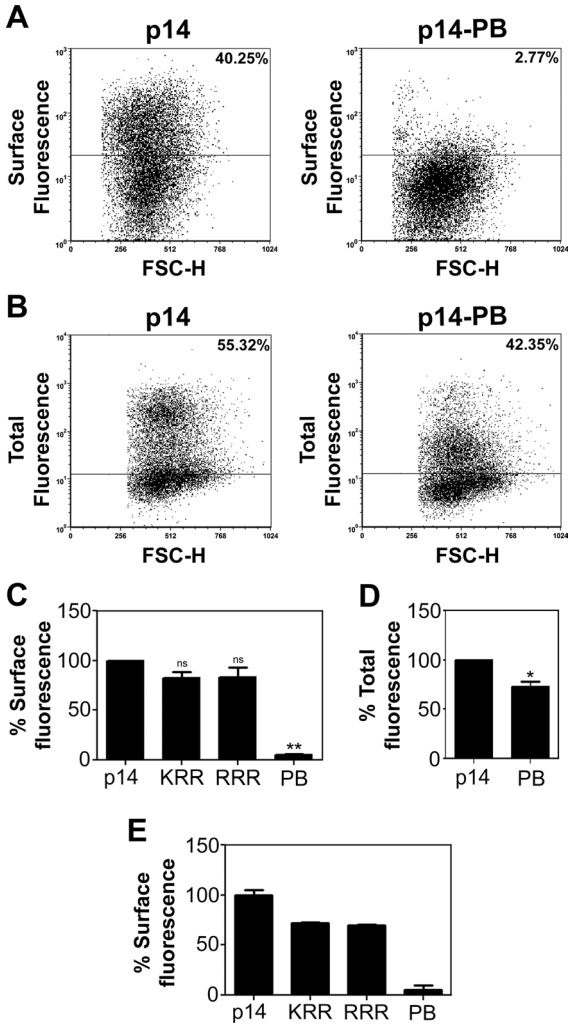

FIGURE 2: The PBM is required for p14 surface expression. (A) QM5 cells transfected with p14 or p14-PB were surface labeled using anti-p14 ectodomain antiserum and Alexa Fluor 647–conjugated secondary antibody, fixed, and analyzed by flow cytometry. Percentage cell surface fluorescence is indicated after background subtraction of empty vector-transfected cells and was determined from the two-dimensional scatter plots of relative fluorescence vs. forward scatter (FSC) using the indicated gating (horizontal line). (B) QM5 cells transfected with p14(G2A) or p14-PB(G2A) were fixed and permeabilized in suspension at 24 hpt. Cells were stained with full-length anti-p14 antiserum, which recognizes both the N-terminal ectodomain and C-terminal endodomain, and Alexa Fluor 647–conjugated secondary antibody. Scatter plots and percentage cell surface fluorescence are shown as in A. (C) Surface fluorescence of QM5 cells transfected with the indicated p14 constructs was quantified as in A. Results are mean percentage cell surface fluorescence ± SEM relative to authentic p14 after background subtraction of empty vector-transfected cells from two independent experiments performed in triplicate. Statistical significance relative to p14 (**$p < 0.01$; ns, not significant). (D) As in C, except that cells were permeabilized before immunostaining to detect total fluorescence of QM5 cells transfected with p14(G2A) and p14-PB(G2A). Results are mean percentage cell fluorescence ± SEM from three independent experiments performed in triplicate. Statistical significance relative to p14 (*$p < 0.05$). (E) As in C, except that cells were stained with an anti-p14 antiserum that recognizes both the N-terminal ectodomain and C-terminal endodomain. Results are mean percentage cell surface fluorescence ± SD relative to authentic p14 for triplicate samples from a single experiment.

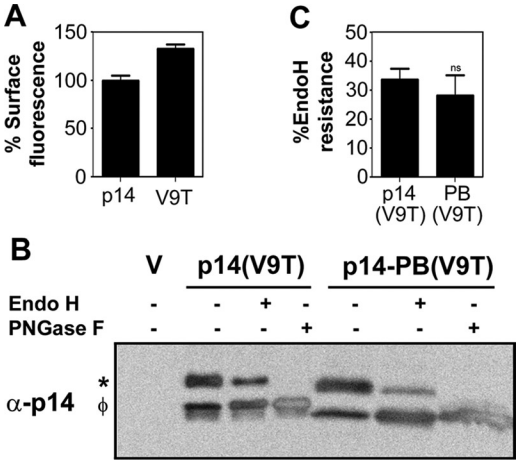

FIGURE 3: The PBM is not required for export of p14 from the ER to the Golgi. (A) QM5 cells transfected with p14 or the nonfusogenic p14(V9T) construct were processed at 24 hpt for cell surface fluorescence by flow cytometry as described in Figure 2A. Results are mean percentage cell surface fluorescence ± SD relative to authentic p14 for triplicate samples from a single experiment. (B) Cell lysates of QM5 cells transfected with empty vector (V), p14(V9T) or p14-PB(V9T) were harvested at 24 hpt, and equal protein amounts were left untreated or treated with endo H or PNGase F, as described in *Materials and Methods*, before Western blotting with anti-p14 antiserum. Left, glycosylated (*) and nonglycosylated (ϕ) p14. (C) Mean percentage of glycosylated p14(V9T) and p14-PB(V9T) that was endo H resistant ± SEM calculated using pixel counts from three independent Western blots as in B. Statistical significance relative to p14 (ns, not significant).

p14(G2A) construct, which displays the same subcellular localization pattern as authentic p14 (Corcoran and Duncan, 2004), instead of the nonfusogenic p14(V9T) construct to ensure that results were reproducible irrespective of the p14 construct. The transferrin receptor, a prototype marker for endocytic recycling, was used as a positive control for dynamin inhibition. Treatment of vector-transfected cells with dynasore inhibited endocytic recycling of the transferrin receptor, as indicated by a dramatic increase in cell surface fluorescence when using a fluorescent transferrin-binding assay (Figure 5, A and D). Treatment of cells with dynasore marginally increased cell surface expression of p14(G2A) (Figure 5C), implying that p14 stably localizes to the plasma membrane and is not subject to rapid endocytic recycling. More important, dynasore did not promote detection of p14-PB(G2A) on the cell surface (Figure 5, B and C). To ensure that dynamin-independent endocytosis did not contribute to the absence of p14-PB plasma membrane localization, we treated cells with anti-p14 antiserum at 37°C for 30 min before fixation, permeabilization, and labeling with a fluorescent secondary antibody. This antibody internalization assay detected only low levels of p14-PB in both premeabilized and nonpermeabilized cells, with no evidence of endocytic antibody uptake or concentration in the Golgi complex (Figure 5E). Endocytic events are thus unlikely to influence Golgi accumulation of p14-PB.

The p14 PBM functions as a tribasic Golgi export signal

To define more clearly the nature of the p14 PBM Golgi export signal, we created 12 additional substitution constructs in the PBM (Figure 6A). When cell surface expression levels of the 15 PBM substitution constructs were rank ordered, there was striking congruence between the number of basic residues and the extent of

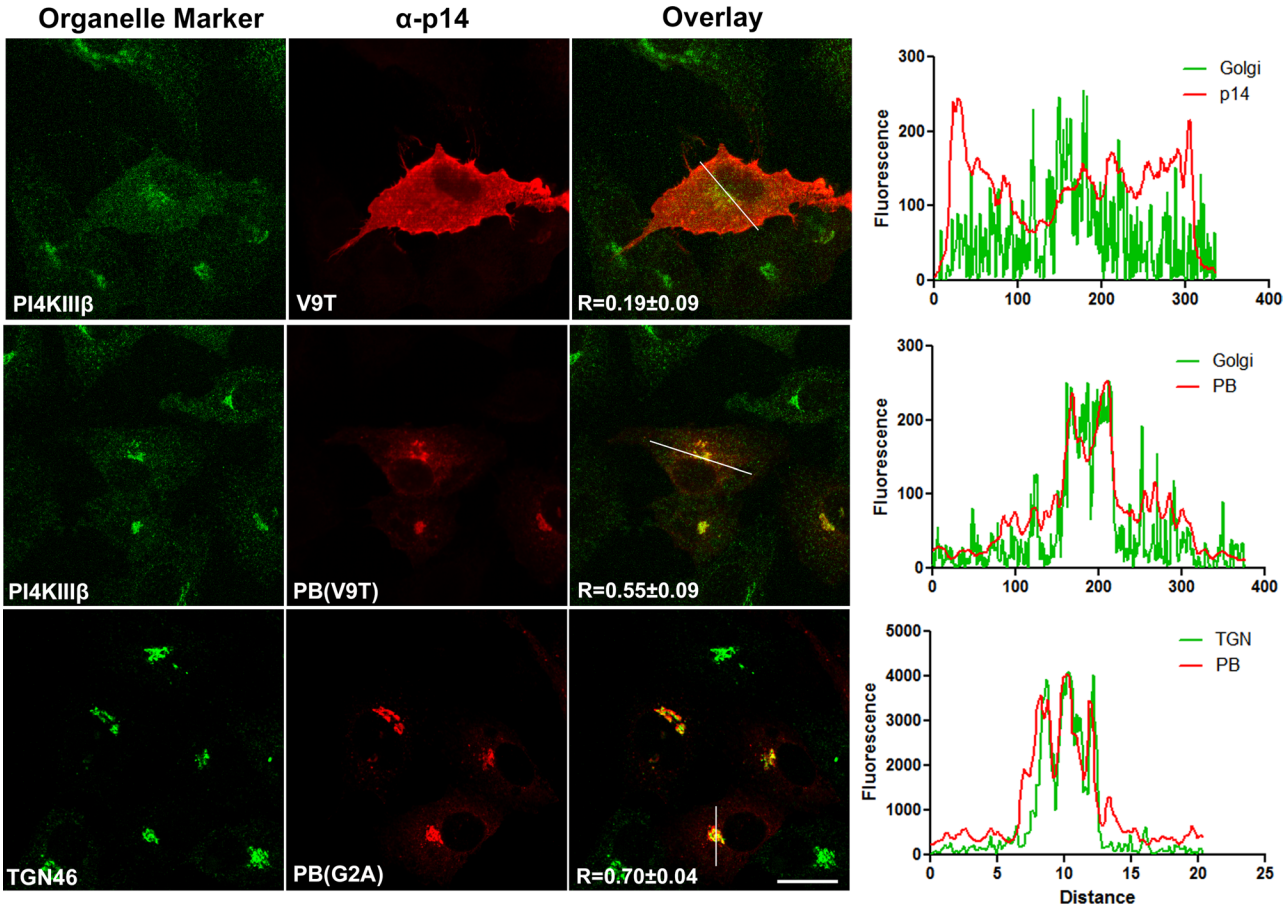

FIGURE 4: Absence of the PBM concentrates p14 in the Golgi complex. Vero cells transfected with p14(G2A) or p14-PB(G2A) were fixed and immunostained at 24 hpt using anti-p14 antiserum (red) and the indicated organelle markers (green) for the Golgi complex (PI4KIIIβ) and TGN (TGN46). Right, merged images. Scale bars, 20 μm. Graphs show relative fluorescence intensities for organelle markers and p14 imaged along the white line in the corresponding merged images, with Pearson's *r* as the mean ± SD from 10 cells indicated on the merged images.

plasma membrane localization, largely independent of specific basic residue locations within the PBM (Figure 6B). The addition of one basic residue to p14-PB increased cell surface fluorescence from <5 to ~20% of p14 levels; two basic residues in any of several locations within the PBM increased cell surface fluorescence to ~40–60%; three or more basic residues exhibited cell surface fluorescence equivalent to p14 with an authentic PBM containing six basic residues (Figure 6B). A one-way analysis of variance (ANOVA) analysis of three independent experiments indicated no significant difference in cell surface expression levels between constructs sharing the same number of basic residues, but differences in cell surface expression were statistically significant between groups (Figure 6B). The substitution results also indicated that it is the number of basic residues, not the net charge of the PBM, that influences Golgi export, since there was no correlation between presence or absence of the acidic Glu residue that separates the two tribasic motifs in the PBM and p14 plasma membrane localization (Figure 6, A and B).

Steady-state total expression levels varied slightly for the different constructs (Figure 6C), with constructs containing fewer than three basic residues consistently showing ~20–40% reduction in steady-state levels by Western blot analysis (Supplemental Figure S1). Decreased steady-state expression is to be expected for plasma membrane proteins that fail to traffic out of the Golgi, since their accumulation would presumably lead to a percentage being trafficked to lysosomes for degradation. The colocalization of p14PB with Golgi complex and TGN markers (Figure 4) also suggests that some of the p14PB proteins that fail to exit the TGN might be retrieved via the COPI pathway. More important, the progressive increase in cell surface expression correlated with increasing number of basic residues (Figure 6B), not with variations in overall expression levels (Supplemental Figure S1). One notable exception to this trend was PB+K,R,R, which contained three basic residues but displayed cell surface fluorescence levels of ~50%, more similar to the levels observed in constructs with two basic charges (Figure 6B). This construct lacked the acidic residue separating the two tribasic motifs, but other constructs lacking this acidic residue were efficiently expressed on the cell surface (e.g., RRE and RER constructs in Figure 6). The basis for this anomaly is unknown, but we note that this was the only construct with three basic residues that did not contain adjacent basic residues. Clustering of basic residues or their spatial arrangement may therefore exert some influence on the function of the PBM as a tribasic Golgi export signal.

The cell surface fluorescence results were confirmed by confocal microscopy of permeabilized cells using representative polybasic

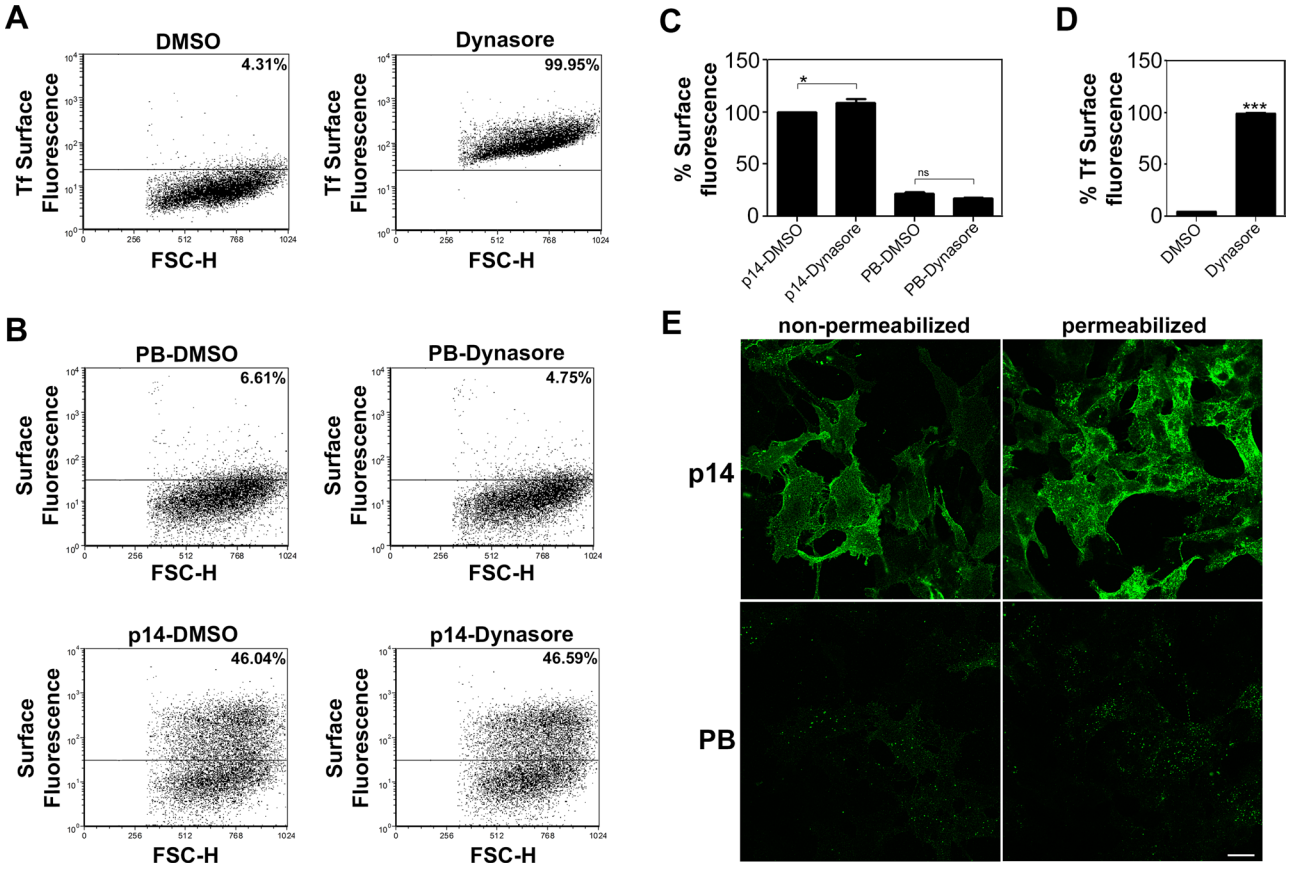

FIGURE 5: Endocytic pathways do not influence plasma membrane localization of p14-PB. (A) Vector-transfected QM5 cells were treated for 1 h in serum-free media with the dynamin inhibitor dynasore (80 µM) at 24 hpt, and live cells were stained using Alexa Fluor 555–conjugated transferrin and analyzed by flow cytometry to detect surface bound transferrin receptor (TfR). Percentage cell surface fluorescence, as in Figure 2A. (B) QM5 cells transfected with p14(G2A) (bottom) or p14-PB(G2A) (top) were treated with DMSO or dynasore as in A. Live cells were stained with anti-p14 ecto antiserum and Alexa Fluor 647–conjugated secondary antibody, and cell surface fluorescence was analyzed by flow cytometry. Percentage cell surface fluorescence, as in Figure 2A. (C) Surface fluorescence of QM5 cells transfected with p14(G2A) or p14-PB(G2A) quantified as in A. Mean percentage cell surface fluorescence ± SEM from three independent experiments performed in triplicate. Statistical significance between the indicated paired samples (*$p < 0.05$; ns, not significant). (D) Transferrin receptor cell surface fluorescence quantified as in B. Mean percentage cell surface fluorescence ± SEM from three independent experiments performed in triplicate (***$p < 0.005$). (E) Vero cells transfected with p14(G2A) or p14-PB(G2A) were incubated with full-length anti-p14 antiserum at 24 hpt for 30 min at 37°C. Cells were then fixed and stained with Alexa Fluor 488-conjugated antibody with (permeabilized) or without (nonpermeabilized) prior Triton X-100 treatment. Scale bar, 20 µm.

mutants in a p14(V9T) backbone. As before, p14-PB(V9T) colocalized extensively with the PI4KIIIβ Golgi marker (Figure 7). Addition of one basic charge (PB+K(V9T)) resulted in a slight increase in diffuse cytoplasmic staining, consistent with FACS results indicating a low level of Golgi export of this construct to the plasma membrane (Figure 6B). Addition of two basic residues further decreased Golgi localization while increasing broadly distributed punctate, cytoplasmic staining (B+K,R(V9T)). Addition of a third basic residue (p14-KRR(V9T)) resulted in little p14 colocalization with the Golgi marker and obvious immunofluorescence staining at the cell periphery, a similar staining pattern as p14(V9T) (Figure 7). Visual results were supported by Pearson's correlation coefficients, which showed a progressive decrease in Golgi colocalization with increasing number of basic residues in the PBM (Figure 7). Efficient p14 trafficking from the Golgi is therefore largely dependent on the presence of three basic residues in the PBM.

Context-dependent effects on the trafficking properties of p14 PBM

Previous studies suggest that the proximity to the TMD of a cytosolic, dibasic ER export signal can influence the function of this trafficking motif (Giraudo and Maccioni, 2003). To determine whether membrane proximity influences the function of the p14 PBM, we appended the p14 PBM to the C-terminus of the p14-PB construct. In this p14-PBextPB construct (Figure 8A), 68 endodomain residues separate the PBM and TMD instead of the four-residue separation in authentic p14. FACS analysis indicated this membrane-distal version of the PBM did not promote trafficking of p14 to the plasma membrane (Figure 8B). To define the nature of the p14-PBextPB trafficking defect, we examined this construct in the p14(V9T) background using the endo H assay. As previously observed, the slower-migrating p14(V9T) polypeptide was completely sensitive to PNGase F but partially resistant to endo H (Figure 8C), indicative of

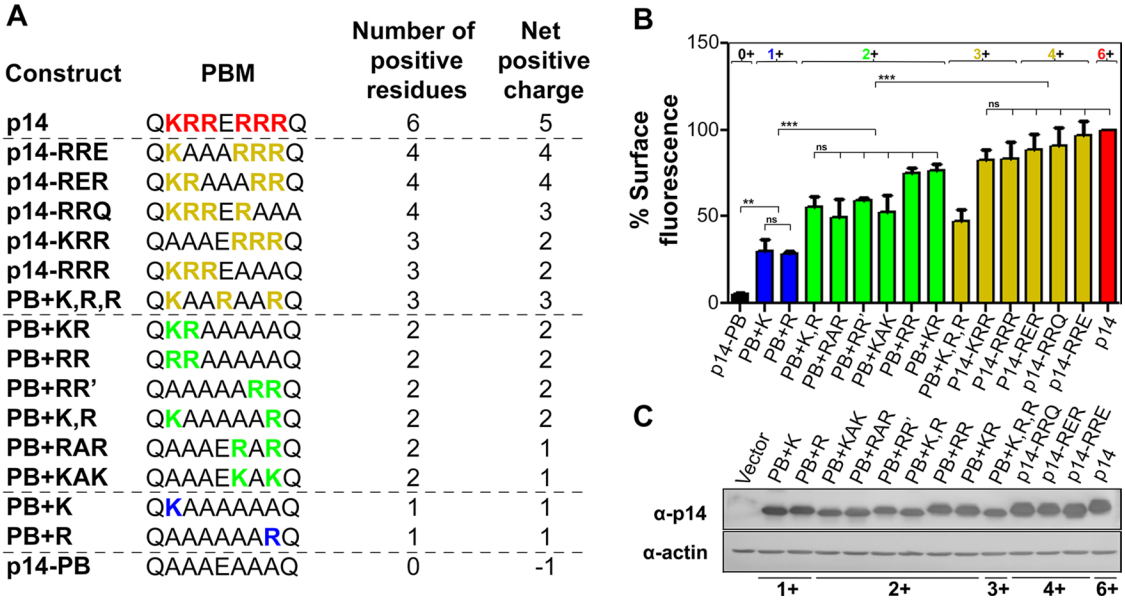

FIGURE 6: Three basic residues are required for maximal p14 cell surface expression. (A) Amino acid sequences of the p14 PBM and the indicated polybasic mutants. The number of positive residues and the net positive charge of the PBM are color coded and indicated. (B) QM5 cells transfected with the indicated p14 constructs were processed for quantification of cell surface fluorescence as described in Figure 2A. Mean percentage cell surface fluorescence ± SEM relative to authentic p14, after background subtraction of empty vector-transfected cells, from three or more independent experiments performed in triplicate. Numbers across the top indicate the number of positive residues present within respective PBMs. One-way ANOVA indicated no significance difference (ns) between constructs sharing the same number of basic residues (except for PB+K,R,R in the 3+ group). Statistical significance between groups (**$p < 0.01$; ***$p < 0.005$). (C) QM5 cells transfected with the indicated p14 constructs were harvested at 8 hpt and processed for Western blotting using anti-p14 antiserum or anti-actin antibody. Numbers at the bottom indicate the number of positive residues present in the PBM.

glycosylation and processing in the Golgi complex to a complex oligosaccharide. In contrast, the glycosylated p14-PBextPB(V9T) polypeptide was completely sensitive to endo H treatment (Figure 8C), suggesting an inability to transit to the Golgi complex. Confocal microscopy also revealed disseminated cytoplasmic staining of p14-PBextPB(V9T) reminiscent of ER staining with no evidence of Golgi localization (Figure 8D), consistent with results from the endo H assay. Thus the proximity of the PBM to the TMD influences its function as a trafficking motif.

The p14 PBM directs Golgi export of a heterologous protein

Results indicated the p14 PBM is necessary for efficient Golgi export of p14, but can it also function to promote Golgi export of a heterologous protein? To address this question, we sought to transfer the PBM to the cytoplasmic tail of a protein that resides in the Golgi complex. Ideally, this heterologous protein should lack a Golgi retention signal that could compete with the Golgi export properties of the p14 PBM. A chimeric ERGIC-53 protein fulfilled these criteria. This protein contains the myc-tagged ectodomain of ERGIC-53 but the TMD of CD4 connected through two Arg residues to a 10-residue polyalanine tail (Gut *et al.*, 1998). The TMD and cytoplasmic tail replacements remove signals that normally retain the ERGIC-53 protein in the early secretory pathway, resulting in preferential localization of the chimeric ERGIC-53 protein to the Golgi complex in stably transfected MDCK cells (Gut *et al.*, 1998). We inserted a sequence corresponding to the p14 membrane-proximal region containing the PBM (KYLQKRRERRRQ) in place of the two Arg residues at the TMD/cytoplasmic tail junction in the chimeric ERGIC-53 construct (Figure 9A). We also constructed a similar replacement with a sequence substituting the basic residues in the p14 PBM with Ala residues (KYLQAAAE-AAAQ). As a positive control for Golgi export of the ERGIC-53 chimera, a second chimeric version of this protein was used that contains two glycosylation sites in the ectodomain, which generates a glycoprotein that is more efficiently exported from the Golgi complex to the plasma membrane (Gut *et al.*, 1998).

All four of the chimeric ERGIC-53 proteins were expressed in stably transfected QM5 cells at approximately equivalent levels, as observed by Western blotting using α-myc antiserum (Figure 9B). As previously reported (Gut *et al.*, 1998), the chimeric ERGIC-53 protein showed reduced levels of cell surface expression when analyzed by flow cytometry, but addition of the glycosylation signals substantially increased plasma membrane localization (Figure 9C). Although the construct containing the p14 PBM region with Ala substitutions had slightly higher levels of cell surface expression than the parental chimeric ERGIC-53 construct, addition of the authentic p14 PBM resulted in cell surface expression at levels equivalent to, or slightly higher than, those induced by glycosylation of the chimeric ERGIC-53 protein (Figure 9C). Immunofluorescence microscopy of stably transfected Vero cells confirmed the cell surface fluorescence results. The parental chimeric ERGIC-53 protein and the construct containing the mutated p14 PBM both displayed strong colocalization with the PI4KIIIβ Golgi complex marker (Figure 10). In contrast, both glycosylated ERGIC-53 protein and the construct containing the p14 PBM displayed disseminated cytoplasmic fluorescence that radiated out to the cell periphery with limited Golgi colocalization (Figure 10). The p14 PBM can therefore function as a

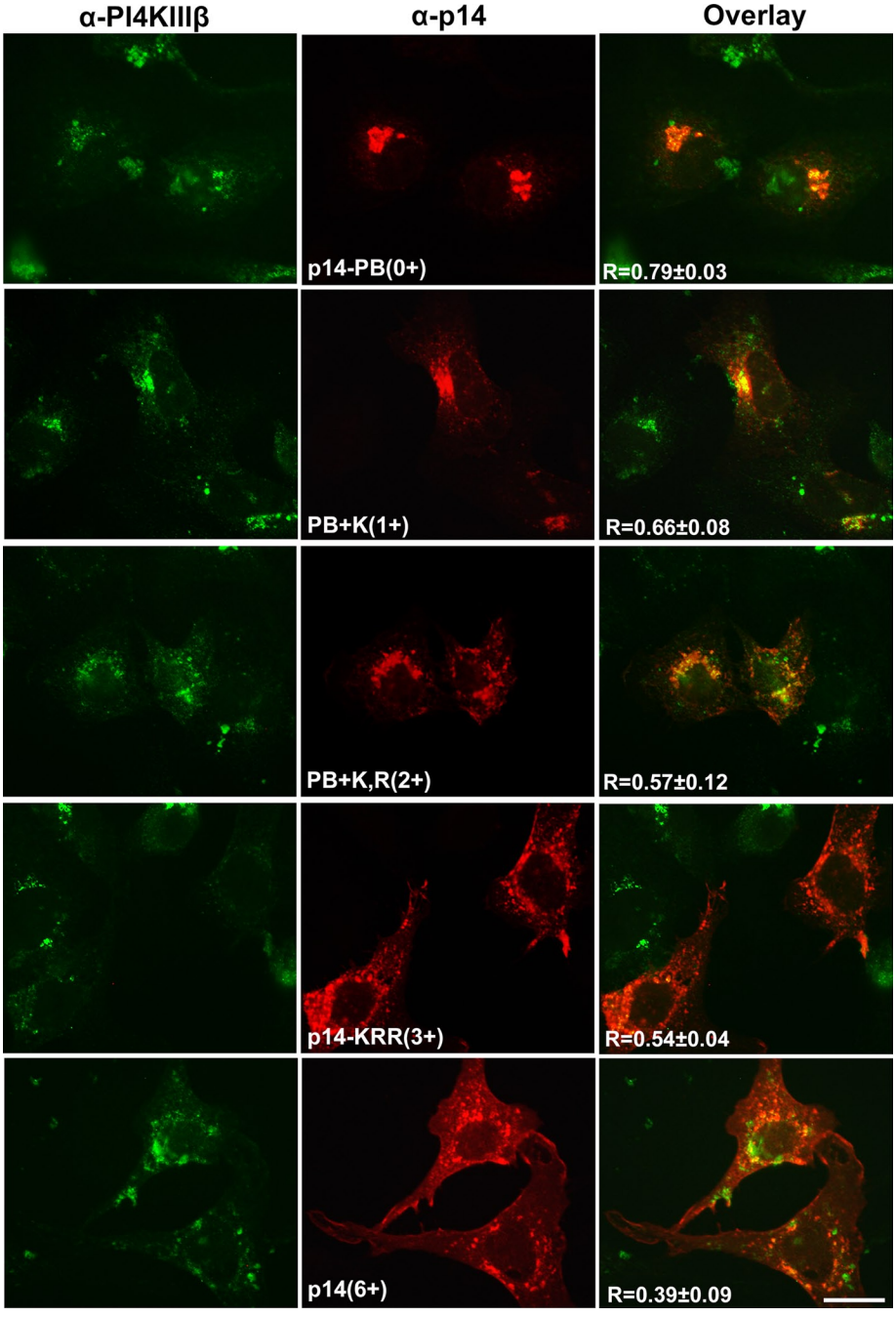

FIGURE 7: Basic residues have an additive effect on p14 Golgi export. Vero cells transfected with p14(V9T) and the indicated p14(V9T) polybasic mutants were immunostained with anti-p14 antiserum (red) and the PI4KIIIβ Golgi marker (green) at 24 hpt. Right, merged images. Pearson's *r* for each construct was calculated for five transfected cells and is shown as mean ± SD. Scale bar, 20 μm.

Golgi export signal to direct Golgi export and plasma membrane trafficking of heterologous proteins.

DISCUSSION

The reovirus FAST proteins are a singular family of virus-encoded fusogens. They are among the smallest of all known membrane fusion proteins, the only examples of nonenveloped virus fusogens, and the only viral membrane fusion proteins whose sole defined function is to induce cell–cell membrane fusion and syncytium formation. Membrane insertion and protein trafficking of the FAST proteins does not involve an N-terminal signal peptide or glycosylation. Plasma membrane localization is therefore dictated by features inherent in the small ectodomains or endodomains of the FAST proteins or their single TMD. The simplified structure and domain organization of these single-pass membrane proteins provide an excellent system to define structure–function determinants for membrane fusion and intracellular protein trafficking. Exploiting the p14 FAST protein to assess plasma membrane localization determinants, we identified a novel Golgi export signal based on a membrane-proximal tribasic motif. Golgi export of p14 is determined by the number of basic residues and not the net positive charge of the cytosolic PBM. Further, the trafficking phenotype was not cell type specific, manifesting the same effects in QM5 fibroblasts and nonpolarized Vero epithelial cells, and the tribasic motif can function as a Golgi export signal or ER retention signal depending on its proximity to the TMD. Of most note, the p14 PBM can mediate efficient export of a heterologous Golgi-resident protein to the plasma membrane. This is the first example of an autonomous Golgi export signal based on a sequence-independent, membrane-proximal tribasic motif.

All FAST proteins contain a cluster of membrane-proximal basic residues whose role in FAST protein–mediated cell–cell fusion is unknown. In the case of the p10 and p15 FAST proteins, these PBMs are essential for cell–cell fusion (Shmulevitz *et al.*, 2003; Dawe *et al.*, 2005). We now show a similar reliance of p14-mediated cell–cell fusion on the presence of the PBM (Figure 1). Previous speculation suggested these PBMs might regulate FAST protein topology in the membrane, since one of the dominant determinants of membrane protein topology is the prevalence of basic residues on the cytosolic side of the TMD (von Heijne, 1989; Nilsson *et al.*, 2005). However, surface immunodetection using an antiserum that recognizes both the N- and C-termini of p14 failed to detect p14-PB in either the correct $N_{lumenal}/C_{cytoplasmic}$ or the inverse $N_{cytoplasmic}/C_{exoplasmic}$ topology on the surface of transfected cells (Figure 2). Furthermore, Ala substitution of the PBM had no negative effect on glycosylation of the p14(V9T) construct (Figure 3). Given that the only N-linked glycosylation site in p14(V9T) is at the introduced Val–Thr substitution nine residues from the N-terminus, p14-PB(V9T) must still assume the correct $N_{lumenal}/C_{cytoplasmic}$ topology. We note that the first residue after the p14 TMD is Lys, which resides four residues upstream of the PBM. This positively charged residue might be sufficient to maintain the normal $N_{lumenal}/C_{cytoplasmic}$ topology of p14 in the absence of the PBM. Thus we demonstrate for the first time that a FAST protein

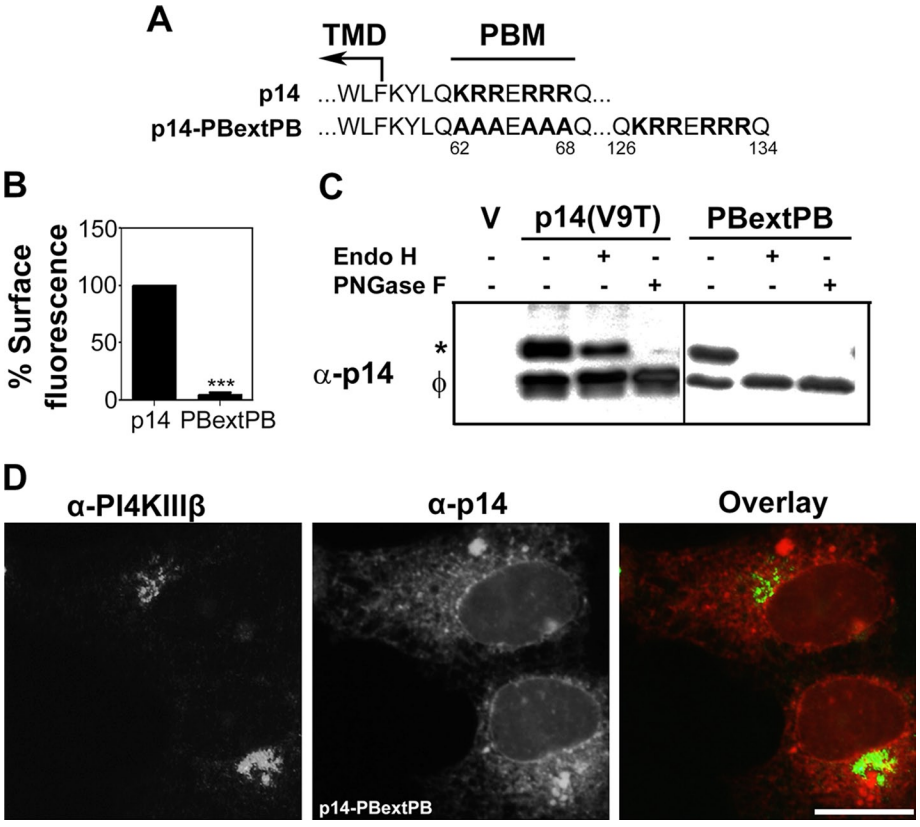

FIGURE 8: Membrane proximity influences the trafficking function of the p14 PBM. (A) Amino acid sequences and location of PBMs in p14 and p14-PBextPB. Numbers indicate residue position in p14. Ile-125 is the C-terminal residue of authentic p14. Boundary of the TMD and location of the PBM are indicated. (B) Percentage cell surface fluorescence analysis of p14 and p14-PBextPB, as described in Figure 2A. Statistical significance relative to p14 (***$p < 0.005$; $n = 3$). (C) Endo H resistance of p14 and p14-PBextPB, as described in Figure 3B. V, empty vector; *glycosylated p14; ϕ, nonglycosylated p14. (D) Vero cells transfected with p14-PBextPB(V9T) and immunostained at 24 hpt using anti-p14 antiserum (red) and the ER marker PDI (green). Right, merged image. Scale bar, 20 μm.

PBM does not affect protein topology in the membrane but is instead essential for localization to the plasma membrane.

Basic residues were identified as sorting signals for ER export to the Golgi complex (Duvernay *et al.*, 2011; Dong *et al.*, 2012), and a membrane-proximal dibasic motif was previously shown to mediate interaction with the Sar1 component of COP II to promote efficient ER exit (Giraudo and Maccioni, 2003). However, several approaches revealed the p14 PBM functions as a membrane-proximal Golgi, not ER, export signal. First, p14 lacking a PBM was exported from ER to the Golgi complex as efficiently as authentic p14, as determined by the percentage of glycosylated p14-PB(V9T) that was endo H-resistant (Figure 3), indicating that the PBM is not required for ER export. Second, immunofluorescence microscopy revealed extensive colocalization of p14-PB with markers of the Golgi complex and TGN (Figure 4), indicating accumulation of p14 in the Golgi complex and TGN when the PBM was removed by Ala substitution. Third, inhibiting dynamin-dependent endocytic pathways had no effect on p14 plasma membrane localization and did not promote detection of p14-PB in the plasma membrane (Figure 5C), whereas an antibody internalization assay failed to detect recycling of p14-PB from the plasma membrane to the Golgi complex (Figure 5E). The most straightforward explanation for these results is the p14 PBM does not function as a plasma membrane retention signal but instead as a Golgi export signal. Finally, moving the p14 PBM from its membrane-proximal location to the C-terminus failed to generate any endo H–resistant glycosylated versions of p14, implying that the p14-PBextPB(V9T) construct failed to traffic from the ER to the Golgi complex (Figure 8). The p14 PBM can therefore function as a Golgi export signal or ER retention signal, depending on its proximity to the TMD.

The effect of membrane proximity on the function of sorting signals was noted previously. For example, the K(X)KXX or [RK](X)[RK] cytosolic motif promotes ER retention or retrieval when located distal from, but not proximal to, the TMD (Vincent *et al.*, 1998). The precise location of two Lys residues in the KKXX motif, at positions –3 and –4 or –5 relative to the C-terminus, is required to allow electrostatic interactions with components of the COPI complex (Jackson *et al.*, 1990, 2012). The p14 PBM does not conform to this consensus arrangement but still promotes ER retention when located at the C-terminus (Figure 8). The [RK](X)[RK] motif promotes ER localization of type II membrane proteins (i.e., N-terminus in the cytosol) using either Lys or Arg residues positioned in one of five possible arrangements relative to the N-terminus (NH_2-XRR, -XXRR, -XXXRR, -XRXR, or -XXRXR; Schutze *et al.*, 1994). Of interest, the p14 PBM contains three of these basic residue arrangements relative to the cytosolic C-terminus (RRX-COOH, RRXX-, and RXRX-). The positioning of diarginine residues relative to the cytosolic termini might therefore mediate ER retention of either type I or type II membrane proteins.

Although sorting signals involved in trafficking from the Golgi complex to various membrane compartments have been described, these motifs function more as sorting signals than export signals per se. Linear, tyrosine- or leucine-based cytosolic signals regulate post-Golgi trafficking in both the biosynthetic and endocytic pathways, targeting proteins to the endosomal/lysosomal compartments (Williams and Fukuda, 1990; Harter and Mellman, 1992; Odorizzi *et al.*, 1994) or basolateral membranes (Hunziker *et al.*, 1991; Matter *et al.*, 1992). Mutating these sorting signals can reduce trafficking efficiency from the Golgi complex to the plasma membrane (Nishimura *et al.*, 2002) but generally leads to mislocalization rather than accumulation in the Golgi (Williams and Fukuda, 1990; Hunziker *et al.*, 1991; Harter and Mellman, 1992; Rajasekaran *et al.*, 1994). As we now show, the p14 PBM functions as a bona fide Golgi export signal. Ala substitutions of all six basic residues decreased plasma membrane localization of p14-PB by >95% (Figure 2B) and resulted in p14-PB accumulation in the Golgi complex (Figure 4). Extensive mutagenic analyses revealed stepwise progressions in Golgi export (Figure 7) and plasma membrane localization (Figure 6) as positively charged residues were reintroduced into p14-PB, reaching maximal levels with three basic residues. Most important, the p14 Golgi export signal was transferable to a heterologous Golgi-resident protein. Addition of the p14 PBM to the ERGIC-53 chimera, but not the Ala-substituted version of

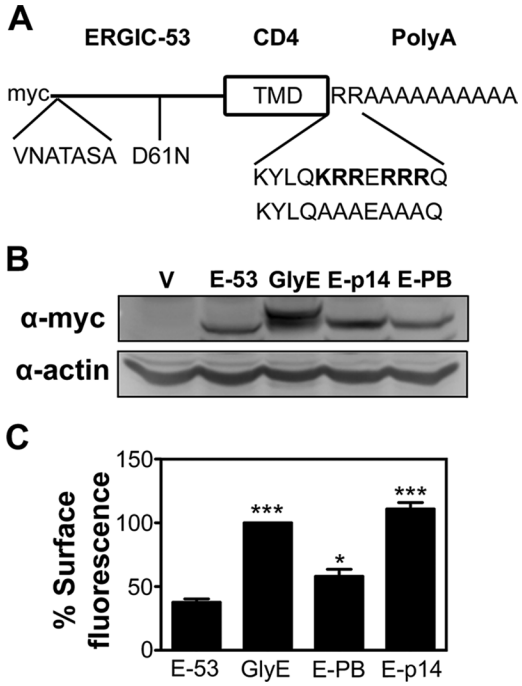

FIGURE 9: p14 PBM traffics a Golgi-resident protein to the plasma membrane. (A) Schematic diagram of the N-terminally myc-tagged chimeric ERGIC-53 protein containing the ERGIC-53 ectodomain, CD4 TMD, and polyalanine (polyA) cytoplasmic tail. The glycosylated ERGIC-53 chimera has two glycosylation sites (VNATASA and D61N) introduced into the ectodomain. The ERGIC-p14 and ERGIC-p14-PB constructs replace the two membrane-proximal endodomain arginine residues in the parental ERGIC-53 chimera with the membrane-proximal p14 sequence containing the PBM (KYLQKRRERRRQ) or the Ala-substituted version of this motif (KYLQAAAEAAAQ). (B) QM5 cells stably transfected with empty vector (V), parental ERGIC-53 chimera (E-53), glycosylated ERGIC-53 chimera (GlyE), ERGIC-53 with the p14 PBM (E-p14), or the Ala-substituted PBM (E-PB) were processed for Western blotting using anti-myc or anti-actin antibody. (C) As in B, except that QM5 cells transfected with the indicated chimeric ERGIC-53 constructs were processed for flow cytometry after live-cell staining with anti-myc antibody and Alexa 647–conjugated secondary antibodies. Mean percentage cell surface fluorescence relative to GlyE transduced cells ± SEM from triplicate samples was calculated from three independent experiments. Statistical significance relative to E-53 (*$p < 0.05$; ***$p < 0.005$).

the PBM, increased cell surface fluorescence (Figure 9) and Golgi export (Figure 10) as efficiently as addition of a glycosylation signal, which was previously reported to promote Golgi export of this construct (Gut *et al.*, 1998). The p14 PBM is therefore sufficient to confer a Golgi export phenotype to an otherwise Golgi-resident protein and promote trafficking to the plasma membrane.

Basic sorting motifs have been well described as ER retention, retrieval, or export signals (Andersson *et al.*, 1999; Giraudo and Maccioni, 2003; Duvernay *et al.*, 2011; Dong *et al.*, 2012), but the p14 PBM is the first example of a Golgi export signal based on a tribasic motif. There is, however, some indication that similar motifs may exist in other proteins. For example, mutation of two basic residues present in the N-terminal cytosolic domain of the bitopic, inward rectifier potassium channel Kir2.1 qualitatively decreases Golgi export to the plasma membrane (Stockklausner and Klocker, 2003). More recent studies indicate these basic residues are part of a bipartite Golgi export signal that includes sequences in the C-terminal cytosolic domain, which are juxtaposed in the tertiary structure (Ma *et al.*, 2011). How the p14 PBM directs Golgi export is unclear, but the present results provide some insights. The PBM is sufficient to direct Golgi export of a heterologous Golgi-resident protein, indicating that, unlike the basic trafficking motif in Kir2.1, it is an autonomous trafficking signal. The Golgi export function of the PBM is also dependent on its close proximity to the membrane. In ER export, membrane-proximal dibasic or tribasic export signals promote interactions with the Sar1 and Sec24C/D components of the COPII complex (Giraudo and Maccioni, 2003; Dong *et al.*, 2012). The requirement for the p14 PBM to be membrane proximal may similarly facilitate interactions with adaptor proteins for Golgi export. However, unlike basic signals involved in ER trafficking, the PBM Golgi export signal is dependent on the number, but not the identity or position, of basic residues. In addition, the relative extent of Golgi export gradually increased with progressive addition of basic residues, implying that additive electrostatic binding promotes Golgi export. These results suggest that electrostatic interactions may not mediate precise interactions with adaptor proteins but instead promote binding to phosphoinositides (PIs). PIs recruit small GTPases, adaptor proteins, and coat proteins to trafficking hubs and promote transport vesicle biogenesis (Santiago-Tirado and Bretscher, 2011). Polybasic clusters have also been shown to concentrate PI in lipid microdomains (Gokhale *et al.*, 2005). It will be interesting to determine whether the p14 PBM preferentially interacts with phosphatidylinositol 4-phosphate or phosphatidylinositol (4,5)-bisphosphate, two PIs involved in Golgi trafficking (De Matteis and Godi, 2004), and whether such interactions recruit p14 to TGN exit sites or lead to generation of Golgi exit sites where p14 resides.

MATERIALS AND METHODS

Cells and antibodies

Vero and QM5 cells were maintained at 37°C and 5% CO_2 in medium 199 with Earle's salts supplemented with 5 or 10% fetal bovine serum (FBS), respectively. The rabbit polyclonal anti-p14 and anti-14 ectodomain antisera were previously described (Corcoran and Duncan, 2004; Top *et al.*, 2005). Antibodies against actin (Sigma-Aldrich, St. Louis, MO), myc epitope tag (Sigma-Aldrich), PI4KIIIβ (BD Biosciences, Franklin Lakes, NJ), TGN46 (Serotec, Oxford, UK), protein disulfide isomerase (PDI; Enzo Life Sciences, Farmingdale, NY), horseradish peroxidase (HRP)–conjugated goat anti-rabbit (Jackson ImmunoResearch, West Grove, PA), Alexa Fluor 488–conjugated goat anti-mouse or donkey anti-sheep, Alexa Fluor 555–conjugated donkey anti-rabbit, and Alexa Fluor 647–conjugated goat anti-rabbit secondary antibodies (Life Technologies, Carlsbad, CA) were obtained from the indicated suppliers.

Cloning and vectors

The p14 gene cloned into pcDNA3 and the nonfusogenic p14(V9T) and p14(G2A) point substitution constructs were described previously (Corcoran and Duncan, 2004). These constructs were used as templates to create the indicated point substitutions in the p14 PBM using the QuikChange (Stratagene, La Jolla, CA) method according to the manufacturer's specifications. The p14PBextPB was created using p14-PB as a template for PCR with a reverse primer that added the PBM to the C-terminus of the protein. The myc-tagged chimeric ERGIC-53 construct with or without glycosylation sites (D61E and VNATASA substitutions in the ectodomain) were provided by Karl Matter (University College London, London, United Kingdom) in the pCB6 vector, subcloned into pcDNA3, and used as templates for PCR with primers that replaced the membrane-proximal diarginine sequence in the cytoplasmic tail with the p14 membrane-proximal

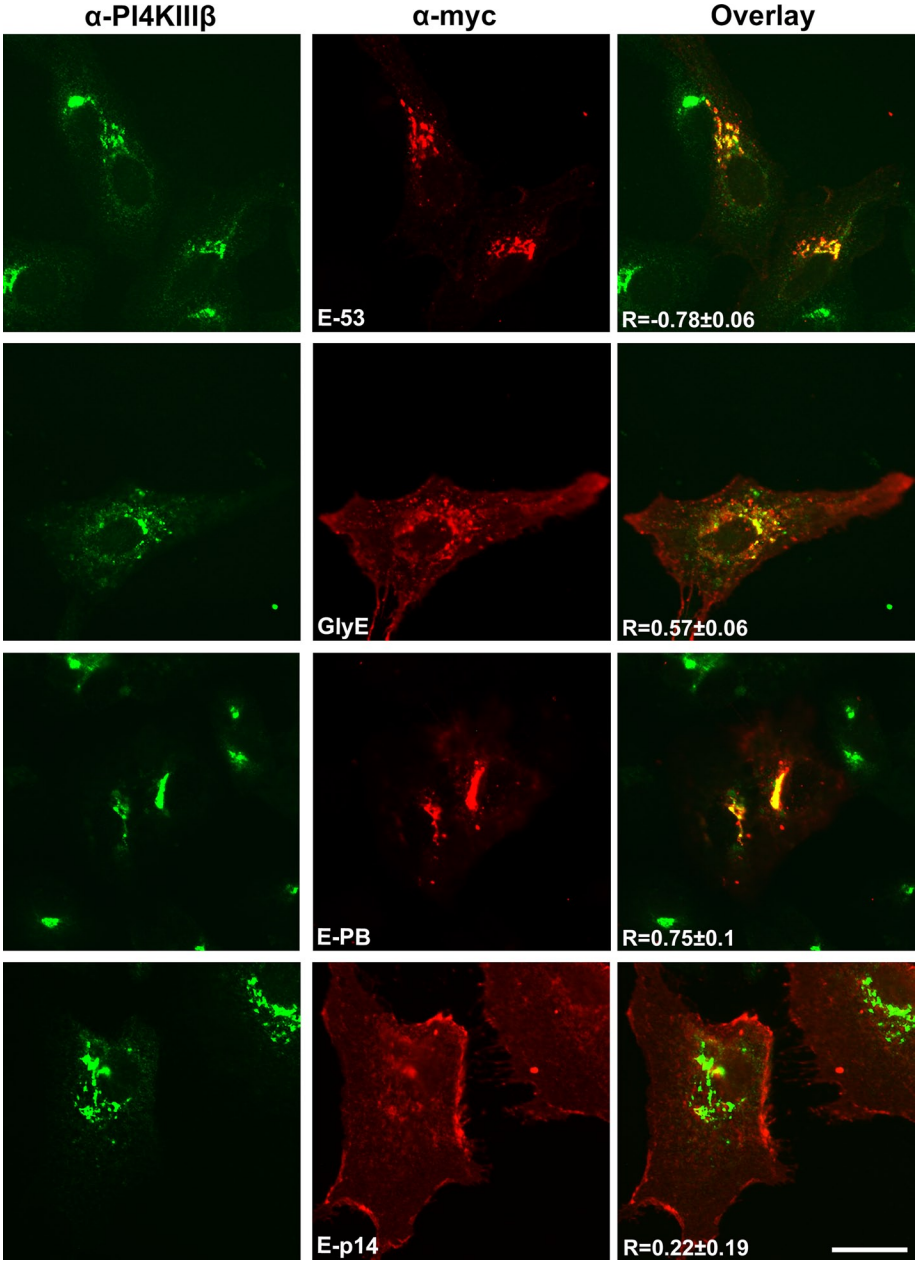

FIGURE 10: The p14 PBM is sufficient to function as a Golgi export signal. Vero cells transfected with the indicated chimeric ERGIC-53 constructs as in Figure 9 were immunostained with anti-myc antibody (red) and the PI4KIIIβ Golgi marker (green). Right, merged images. Pearson's *r* is shown in the merged images of each construct as the mean ± SD from nine cells. Scale bars, 20 μm.

region containing the PBM (KYLQKRRERRRQ) or Ala substitutions of the PBM (KYLQAAAEAAAQ). All experiments were performed using transient transfections with these vectors, except for the ERGIC-53 chimeras that were used in stably transfected cells.

Transfection and syncytial indexing

Cluster plates containing subconfluent monolayers of QM5 or Vero cells were transfected with expression plasmids using Lipofectamine (Invitrogen) or jetPRIME (PolyPlus Transfection, Illkirch, France), respectively, according to the manufacturer's instructions. At 8 hpt the QM5 monolayers were rinsed with Hank's balanced salt solution (HBSS), fixed with methanol, and stained using Wright–Giemsa stain, and a syncytial index was determined by counting the number of syncytial nuclei (i.e., cells containing >4 nuclei/cell) in five random microscopic fields, as previously described (Corcoran and Duncan, 2004). For stable transfections with the ERGIC-53 constructs, at 24 hpt the growth medium on QM5 or Vero cells was replaced with growth medium containing 1 mg/ml G418 (Life Technologies), and transfected cells were cultured under these selective conditions for 5 d with subculturing in the selective medium as required.

Western blotting

At 8 hpt, QM5 cells were lysed with RIPA buffer (50 mM Tris, pH 8.0, 150 mM NaCl, 1 mM EDTA, 1% NP-40, 0.5% IGEPAL) containing 1 μM protease inhibitors (aprotinin, pepstatin, and leupeptin) for 45 min on ice. Equivalent protein loads, as determined by Lowry assays (Bio-Rad, Hercules, CA), were analyzed by SDS–PAGE (15% acrylamide) and Western blotting using anti-p14 antiserum (1:10,000) or antibodies against actin (1:2500) or the myc epitope tag (1:2500) and a HRP-conjugated goat anti-rabbit secondary antibody (1:10,000). For the endo H assays, cells were lysed at 24 hpt, and before SDS–PAGE lysates were treated at 37˚C for 2 h with endo H or PNGase F according to the manufacturer's specifications (New England BioLabs, Ipswich, MA). Membranes were developed using ECL-Plus reagent (GE Healthcare, Little Chalfont, UK) and imaged on a Typhoon 9410 variable-mode imager (GE Healthcare) or a Kodak 4000-mm Pro CCD imager. Blots were quantified by ImageJ (National Institutes of Health, Bethesda, MD) and results reported as band intensity relative to authentic p14.

Cell surface immunofluorescence flow cytometry

Transfected QM5 cells were cultured for 24 h in growth medium containing a 1:20 dilution of anti-p14 ectodomain antiserum to prevent syncytium formation. Conversely, cells transfected with the nonfusogenic p14(G2A) pr p14(V9T) constructs were cultured for 24 h in normal growth medium. Live cells were then incubated at 4˚C for 30 min in blocking buffer (5% normal goat serum, 1% bovine serum albumin, 0.02% NaN_3 in HBSS) and stained with a 1:1000 dilution of anti-p14 ectodomain, anti-14 full length antiserum, or anti-myc antibody (for the chimeric ERGIC-53 constructs) and a 1:2000 dilution of Alexa 647–conjugated goat anti-rabbit secondary antibody, each for 1 h at 4˚C. Cells were resuspended in phosphate-buffered saline (PBS) containing 10 mM EDTA and fixed with 3.7% formaldehyde, and 10,000 cells were analyzed by flow cytometry (FACSCalibur; BD Biosciences) using De-Novo software. Cells transfected with empty vector were used as negative controls for immunostaining, the fluorescence gate was set to

<5%, and the same gate was applied to quantify surface fluorescence of the p14-transfected cells. Background fluorescence from vector-transfected cells was subtracted before mean percentage surface fluorescence was calculated.

Intracellular immunofluorescence flow cytometry

QM5 cells were transfected with nonfusogenic p14(G2A) or p14-PB(G2A) for 24 h in normal culture medium. Cells were then resuspended in PBS with 10 mM EDTA and fixed with 1% paraformaldehyde in PBS for 15 min at room temperature. Cells were pelleted, washed with PBS, and permeabilized in blocking buffer containing 0.1% saponin for 30 min at room temperature. Cells were then labeled with 1:1000 dilution of anti-p14 antiserum and 1:2000 dilution of Alexa 647–conjugated goat anti-rabbit secondary antibody, each for 1 h at room temperature in blocking buffer containing 0.1% saponin. Cells were resuspended in PBS and analyzed by flow cytometry as indicated for cell surface immunofluorescence.

Intracellular immunofluorescence microscopy

At 24 hpt, transfected Vero cells cultured on glass coverslips (Thermo Scientific, Hampton, NH) were fixed in 3.7% formaldehyde for 20 min at room temperature, permeabilized for 20 min at room temperature with 0.1% Triton X-100, blocked for 30 min in blocking buffer, and stained with rabbit anti-p14 antiserum (1:200) or rabbit anti-myc antibodies (1:1000) or with 1:1000 dilutions of mouse monoclonal antibodies against a Golgi marker (PI4KIIIβ), TGN marker (TGN46), or ER marker (PDI) and with 1:1000 dilutions of Alexa 488–conjugated goat anti-mouse or Alexa 647–conjugated goat anti-rabbit secondary antibodies. Coverslips were mounted on glass slides using fluorescence mounting medium (Dako, Glostrup, Denmark) or Prolong gold antifade reagent (Life Technologies) and then visualized and photographed using a Zeiss LSM 510 META confocal microscope or a Zeiss Axioplan II MOT and AxioCam HRC Color Camera. Images were acquired with either 63 or 100× objective. Images were analyzed by ImageJ to generate fluorescence intensity graphs. Pearson's *r* was determined for 5–10 cells on unadjusted images using the Fiji version of ImageJ (Schindelin *et al.*, 2012). If required, background was corrected using the rolling ball background plug-in, and colocalization thresholds were set using the Coloc_2 plug-in (Costes *et al.*, 2004).

Endocytosis inhibition assay

Cells were transfected with nonfusogenic p14(G2A) or p14-PB(G2A), and at 24 hpt, cells were incubated with 80 μM dynasore (Santa Cruz Biotechnology, Dallas, TX) or 0.8% dimethyl sulfoxide (DMSO; Sigma-Aldrich) at 37˚C for 1 h in serum-free growth medium. Cells were then treated and analyzed for p14 surface expression as described in surface expression assay. For analyzing dynasore functionality, vector-transfected cells were serum starved for 30 min and then incubated with 80 μM dynasore or 0.8% DMSO at 37˚C for 30 min. Alexa 555–conjugated transferrin (Molecular Probes) was then added (20 μg/ml) to cells for 20 min at 4˚C. Cells were then harvested and analyzed as described in surface expression assay.

Antibody internalization assay

Vero cells cultured on glass coverslips were transfected with nonfusogenic p14(G2A) or p14-PB(G2A) and incubated for 24 h with normal growth medium. Cells were then incubated with blocking buffer and subsequently with 1:200 dilution of anti-p14 antiserum in blocking buffer, each for 30 min at 37C. Cells were fixed with 4% paraformaldehyde for 15 min at room temperature and then processed further as nonpermeabilized cells or after permeabilization with 0.1% Triton X-100 in PBS for 15 min at room temperature using Alexa Fluor 488–conjugated goat anti-rabbit antibody, as described for 1 h at room temperature. Coverslips were then mounted and analyzed as indicated in intracellular immunofluorescence staining.

Statistical analysis

Statistical analysis and sample comparison were performed using Prism software (GraphPad, San Diego, CA). Groups of two samples were analyzed with a paired two-tailed *t* test, and groups of more than two samples were analyzed using ANOVA with a Tukey post test.

ACKNOWLEDGMENTS

We indebted to Karl Matter (University College, London, United Kingdom) for providing the ERGIC-53 and ERGIC-53 glycosylated chimeric clones and for very helpful discussions on the use of these clones and to Craig McCormick (Dalhousie, Halifax, Canada) and Neale Ridgway (Dalhousie) for providing antibodies and reagents. This work was funded by grants to R.D. from the Natural Sciences and Engineering Research Council of Canada and the Canadian Institutes of Health Research. C.B. was supported by a scholarship from the Nova Scotia Health Research Foundation, and C.B. and F.K. were supported by scholarships from the Cancer Research Training Program with funding from the Dalhousie Cancer Research Program.

REFERENCES

Almen MS, Nordstrom KJ, Fredriksson R, Schioth HB (2009). Mapping the human membrane proteome: a majority of the human membrane proteins can be classified according to function and evolutionary origin. BMC Biol 7, 50.

Andersson H, Kappeler F, Hauri HP (1999). Protein targeting to endoplasmic reticulum by dilysine signals involves direct retention in addition to retrieval. J Biol Chem 274, 15080–15084.

Anitei M, Hoflack B (2011). Exit from the *trans*-Golgi network: from molecules to mechanisms. Curr Opin Cell Biol 23, 443–451.

Barlowe C (2003). Signals for COPII-dependent export from the ER: what's the ticket out? Trends Cell Biol 13, 295–300.

Barry C, Duncan R (2009). Multifaceted sequence-dependent and -independent roles for reovirus FAST protein cytoplasmic tails in fusion pore formation and syncytiogenesis. J Virol 83, 12185–12195.

Barry C, Key T, Haddad R, Duncan R (2010). Features of a spatially constrained cystine loop in the p10 FAST protein ectodomain define a new class of viral fusion peptides. J Biol Chem 285, 16424–16433.

Bonifacino JS, Traub LM (2003). Signals for sorting of transmembrane proteins to endosomes and lysosomes. Annu Rev Biochem 72, 395–447.

Boutilier J, Duncan R (eds.) (2011). The Reovirus Fusion-Associated Small Transmembrane (FAST) Proteins: Virus-Encoded Cellular Fusogens, New York: Elsevier.

Clancy EK, Duncan R (2009). Reovirus FAST protein transmembrane domains function in a modular, primary sequence-independent manner to mediate cell-cell membrane fusion. J Virol 83, 2941–2950.

Corcoran JA, Clancy EK, Duncan R (2011). Homomultimerization of the reovirus p14 fusion-associated small transmembrane protein during transit through the ER-Golgi complex secretory pathway. J Gen Virol 92, 162–166.

Corcoran JA, Duncan R (2004). Reptilian reovirus utilizes a small type III protein with an external myristylated amino terminus to mediate cell-cell fusion. J Virol 78, 4342–4351.

Costes SV, Daelemans D, Cho EH, Dobbin Z, Pavlakis G, Lockett S (2004). Automatic and quantitative measurement of protein-protein colocalization in live cells. Biophys J 86, 3993–4003.

Dawe S, Corcoran JA, Clancy EK, Salsman J, Duncan R (2005). Unusual topological arrangement of structural motifs in the baboon reovirus fusion-associated small transmembrane protein. J Virol 79, 6216–6226.

Dawe S, Duncan R (2002). The S4 genome segment of baboon reovirus is bicistronic and encodes a novel fusion-associated small transmembrane protein. J Virol 76, 2131–2140.

De Matteis MA, Godi A (2004). PI-loting membrane traffic. Nat Cell Biol 6, 487–492.

De Matteis MA, Luini A (2008). Exiting the Golgi complex. Nat Rev Mol Cell Biol 9, 273–284.
Dong C, Nichols CD, Guo J, Huang W, Lambert NA, Wu G (2012). A triple Arg motif mediates alpha(2B)-adrenergic receptor interaction with Sec24C/D and export. Traffic 13, 857–868.
Duncan R (1999). Extensive sequence divergence and phylogenetic relationships between the fusogenic and nonfusogenic orthoreoviruses: a species proposal. Virology 260, 316–328.
Duvernay MT, Dong C, Zhang X, Zhou F, Nichols CD, Wu G (2009). Anterograde trafficking of G protein-coupled receptors: function of the C-terminal F(X)6LL motif in export from the endoplasmic reticulum. Mol Pharmacol 75, 751–761.
Duvernay MT, Wang H, Dong C, Guidry JJ, Sackett DL, Wu G (2011). Alpha2B-adrenergic receptor interaction with tubulin controls its transport from the endoplasmic reticulum to the cell surface. J Biol Chem 286, 14080–14089.
Farhan H, Reiterer V, Korkhov VM, Schmid JA, Freissmuth M, Sitte HH (2007). Concentrative export from the endoplasmic reticulum of the gamma-aminobutyric acid transporter 1 requires binding to SEC24D. J Biol Chem 282, 7679–7689.
Giraudo CG, Maccioni HJ (2003). Endoplasmic reticulum export of glycosyltransferases depends on interaction of a cytoplasmic dibasic motif with Sar1. Mol Biol Cell 14, 3753–3766.
Gokhale NA, Abraham A, Digman MA, Gratton E, Cho W (2005). Phosphoinositide specificity of and mechanism of lipid domain formation by annexin A2-p11 heterotetramer. J Biol Chem 280, 42831–42840.
Guo H, Sun X, Yan L, Shao L, Fang Q (2013). The NS16 protein of aquareovirus-C is a fusion-associated small transmembrane (FAST) protein, and its activity can be enhanced by the nonstructural protein NS26. Virus Res 171, 129–137.
Gurkan C, Stagg SM, Lapointe P, Balch WE (2006). The COPII cage: unifying principles of vesicle coat assembly. Nat Rev Mol Cell Biol 7, 727–738.
Gut A, Kappeler F, Hyka N, Balda MS, Hauri HP, Matter K (1998). Carbohydrate-mediated Golgi to cell surface transport and apical targeting of membrane proteins. EMBO J 17, 1919–1929.
Harter C, Mellman I (1992). Transport of the lysosomal membrane glycoprotein lgp120 (lgp-A) to lysosomes does not require appearance on the plasma membrane. J Cell Biol 117, 311–325.
Hofherr A, Fakler B, Klocker N (2005). Selective Golgi export of Kir2.1 controls the stoichiometry of functional Kir2.x channel heteromers. J Cell Sci 118, 1935–1943.
Hunziker W, Harter C, Matter K, Mellman I (1991). Basolateral sorting in MDCK cells requires a distinct cytoplasmic domain determinant. Cell 66, 907–920.
Jackson LP, Lewis M, Kent HM, Edeling MA, Evans PR, Duden R, Owen DJ (2012). Molecular basis for recognition of dilysine trafficking motifs by COPI. Dev Cell 23, 1255–1262.
Jackson MR, Nilsson T, Peterson PA (1990). Identification of a consensus motif for retention of transmembrane proteins in the endoplasmic reticulum. EMBO J 9, 3153–3162.
Kirchhausen T, Macia E, Pelish HE (2008). Use of dynasore, the small molecule inhibitor of dynamin, in the regulation of endocytosis. Methods Enzymol 438, 77–93.
Ma D, Taneja TK, Hagen BM, Kim BY, Ortega B, Lederer WJ, Welling PA (2011). Golgi export of the Kir2.1 channel is driven by a trafficking signal located within its tertiary structure. Cell 145, 1102–1115.
Matter K, Hunziker W, Mellman I (1992). Basolateral sorting of LDL receptor in MDCK cells: the cytoplasmic domain contains two tyrosine-dependent targeting determinants. Cell 71, 741–753.
Miller EA, Beilharz TH, Malkus PN, Lee MC, Hamamoto S, Orci L, Schekman R (2003). Multiple cargo binding sites on the COPII subunit Sec24p ensure capture of diverse membrane proteins into transport vesicles. Cell 114, 497–509.
Nilsson J, Persson B, von Heijne G (2005). Comparative analysis of amino acid distributions in integral membrane proteins from 107 genomes. Proteins 60, 606–616.
Nishimura N, Balch WE (1997). A di-acidic signal required for selective export from the endoplasmic reticulum. Science 277, 556–558.
Nishimura N, Bannykh S, Slabough S, Matteson J, Altschuler Y, Hahn K, Balch WE (1999). A di-acidic (DXE) code directs concentration of cargo during export from the endoplasmic reticulum. J Biol Chem 274, 15937–15946.
Nishimura N, Plutner H, Hahn K, Balch WE (2002). The delta subunit of AP-3 is required for efficient transport of VSV-G from the trans-Golgi network to the cell surface. Proc Natl Acad Sci USA 99, 6755–6760.
Nufer O, Kappeler F, Guldbrandsen S, Hauri HP (2003). ER export of ERGIC-53 is controlled by cooperation of targeting determinants in all three of its domains. J Cell Sci 116, 4429–4440.
Odorizzi CG, Trowbridge IS, Xue L, Hopkins CR, Davis CD, Collawn JF (1994). Sorting signals in the MHC class II invariant chain cytoplasmic tail and transmembrane region determine trafficking to an endocytic processing compartment. J Cell Biol 126, 317–330.
Pandey KN (2010). Small peptide recognition sequence for intracellular sorting. Curr Opin Biotechnol 21, 611–620.
Racine T, Hurst T, Barry C, Shou J, Kibenge F, Duncan R (2009). Aquareovirus effects syncytiogenesis by using a novel member of the FAST protein family translated from a noncanonical translation start site. J Virol 83, 5951–5955.
Rajasekaran AK, Humphrey JS, Wagner M, Miesenbock G, Le Bivic A, Bonifacino JS, Rodriguez-Boulan E (1994). TGN38 recycles basolaterally in polarized Madin-Darby canine kidney cells. Mol Biol Cell 5, 1093–1103.
Rodriguez-Boulan E, Musch A (2005). Protein sorting in the Golgi complex: shifting paradigms. Biochim Biophys Acta 1744, 455–464.
Salsman J, Top D, Boutilier J, Duncan R (2005). Extensive syncytium formation mediated by the reovirus FAST proteins triggers apoptosis-induced membrane instability. J Virol 79, 8090–8100.
Santiago-Tirado FH, Bretscher A (2011). Membrane-trafficking sorting hubs: cooperation between PI4P and small GTPases at the *trans*-Golgi network. Trends Cell Biol 21, 515–525.
Schindelin J *et al*. (2012). Fiji: an open-source platform for biological-image analysis. Nat Methods 9, 676–682.
Schutze MP, Peterson PA, Jackson MR (1994). An N-terminal double-arginine motif maintains type II membrane proteins in the endoplasmic reticulum. EMBO J 13, 1696–1705.
Sevier CS, Weisz OA, Davis M, Machamer CE (2000). Efficient export of the vesicular stomatitis virus G protein from the endoplasmic reticulum requires a signal in the cytoplasmic tail that includes both tyrosine-based and di-acidic motifs. Mol Biol Cell 11, 13–22.
Shmulevitz M, Corcoran J, Salsman J, Duncan R (2004). Cell-cell fusion induced by the avian reovirus membrane fusion protein is regulated by protein degradation. J Virol 78, 5996–6004.
Shmulevitz M, Duncan R (2000). A new class of fusion-associated small transmembrane (FAST) proteins encoded by the non-enveloped fusogenic reoviruses. EMBO J 19, 902–912.
Shmulevitz M, Salsman J, Duncan R (2003). Palmitoylation, membrane-proximal basic residues, and transmembrane glycine residues in the reovirus p10 protein are essential for syncytium formation. J Virol 77, 9769–9779.
Stagg SM, LaPointe P, Razvi A, Gurkan C, Potter CS, Carragher B, Balch WE (2008). Structural basis for cargo regulation of COPII coat assembly. Cell 134, 474–484.
Stockklausner C, Klocker N (2003). Surface expression of inward rectifier potassium channels is controlled by selective Golgi export. J Biol Chem 278, 17000–17005.
Thalmann CM, Cummins DM, Yu M, Lunt R, Pritchard LI, Hansson E, Crameri S, Hyatt A, Wang LF (2010). Broome virus, a new fusogenic *Orthoreovirus* species isolated from an Australian fruit bat. Virology 402, 26–40.
Top D, de Antueno R, Salsman J, Corcoran J, Mader J, Hoskin D, Touhami A, Jericho MH, Duncan R (2005). Liposome reconstitution of a minimal protein-mediated membrane fusion machine. EMBO J 24, 2980–2988.
Vincent MJ, Martin AS, Compans RW (1998). Function of the KKXX motif in endoplasmic reticulum retrieval of a transmembrane protein depends on the length and structure of the cytoplasmic domain. J Biol Chem 273, 950–956.
von Heijne G (1989). Control of topology and mode of assembly of a polytopic membrane protein by positively charged residues. Nature 341, 456–458.
Votsmeier C, Gallwitz D (2001). An acidic sequence of a putative yeast Golgi membrane protein binds COPII and facilitates ER export. EMBO J 20, 6742–6750.
Williams MA, Fukuda M (1990). Accumulation of membrane glycoproteins in lysosomes requires a tyrosine residue at a particular position in the cytoplasmic tail. J Cell Biol 111, 955–966.
Zanetti G, Pahuja KB, Studer S, Shim S, Schekman R (2011). COPII and the regulation of protein sorting in mammals. Nat Cell Biol 14, 20–28.
Zhang X, Dong C, Wu QJ, Balch WE, Wu G (2011). Di-acidic motifs in the membrane-distal C termini modulate the transport of angiotensin II receptors from the endoplasmic reticulum to the cell surface. J Biol Chem 286, 20525–20535.
Zimmermann R, Eyrisch S, Ahmad M, Helms V (2011). Protein translocation across the ER membrane. Biochim Biophys Acta 1808, 912–924.